

Supporting Information

Growth-driven displacement of protein aggregates along the cell length ensures partitioning to both daughter cells in *Caulobacter crescentus*

Frederic D. Schramm[†], Kristen Schroeder[†], Jonatan Alvelid, Ilaria Testa and Kristina Jonas

[†] Equal contribution

Content

Supporting Information Fig. S1.

Supporting Information Fig. S2.

Supporting Information Fig. S3.

Supporting Information Fig. S4.

Supporting Information Fig. S5.

Supporting Information Fig. S6.

Supporting Information Fig. S7.

Supporting Information Fig. S8.

Supporting Information Fig. S9.

Supporting Information - Strain Construction

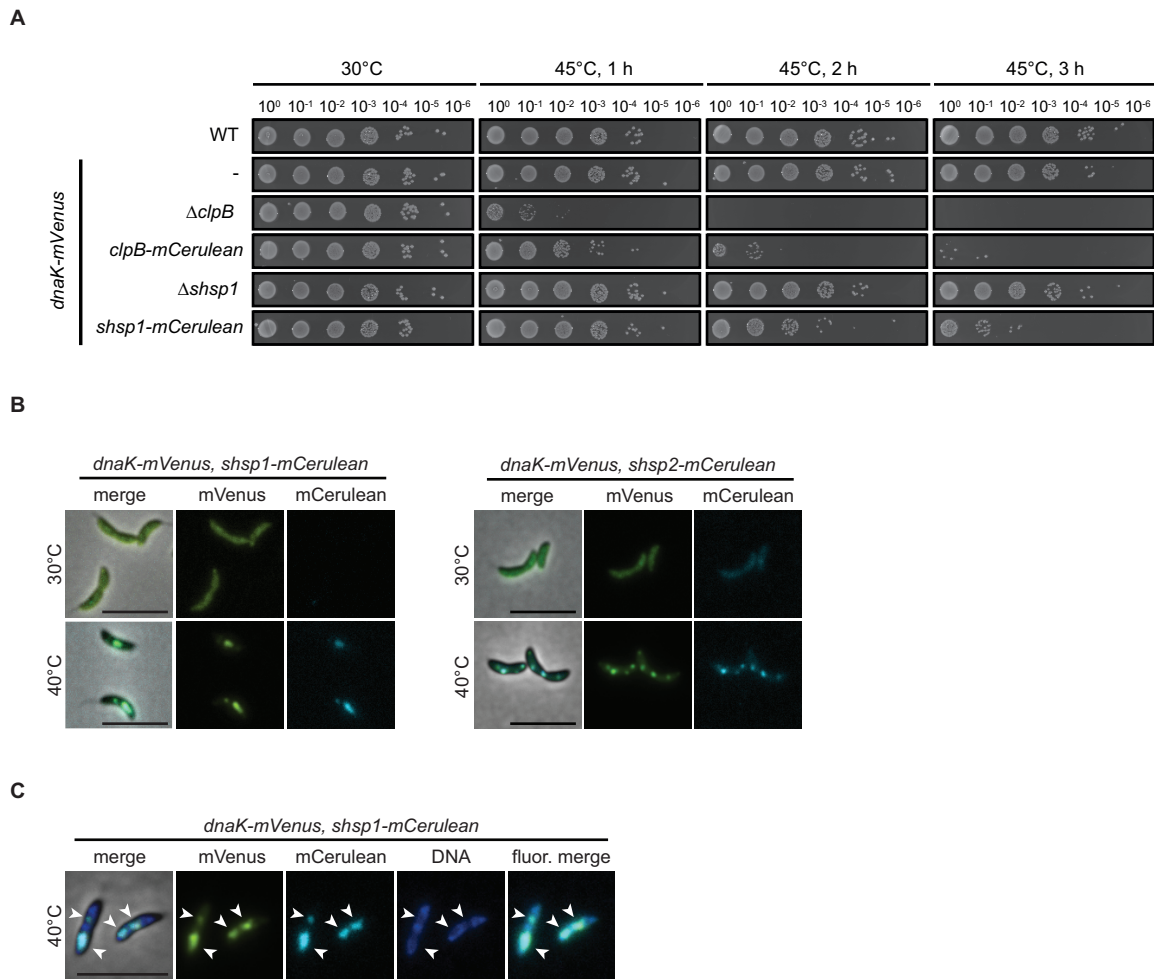
Supporting Information References

Additional Supporting Information Files:

Supporting Information Table S1.

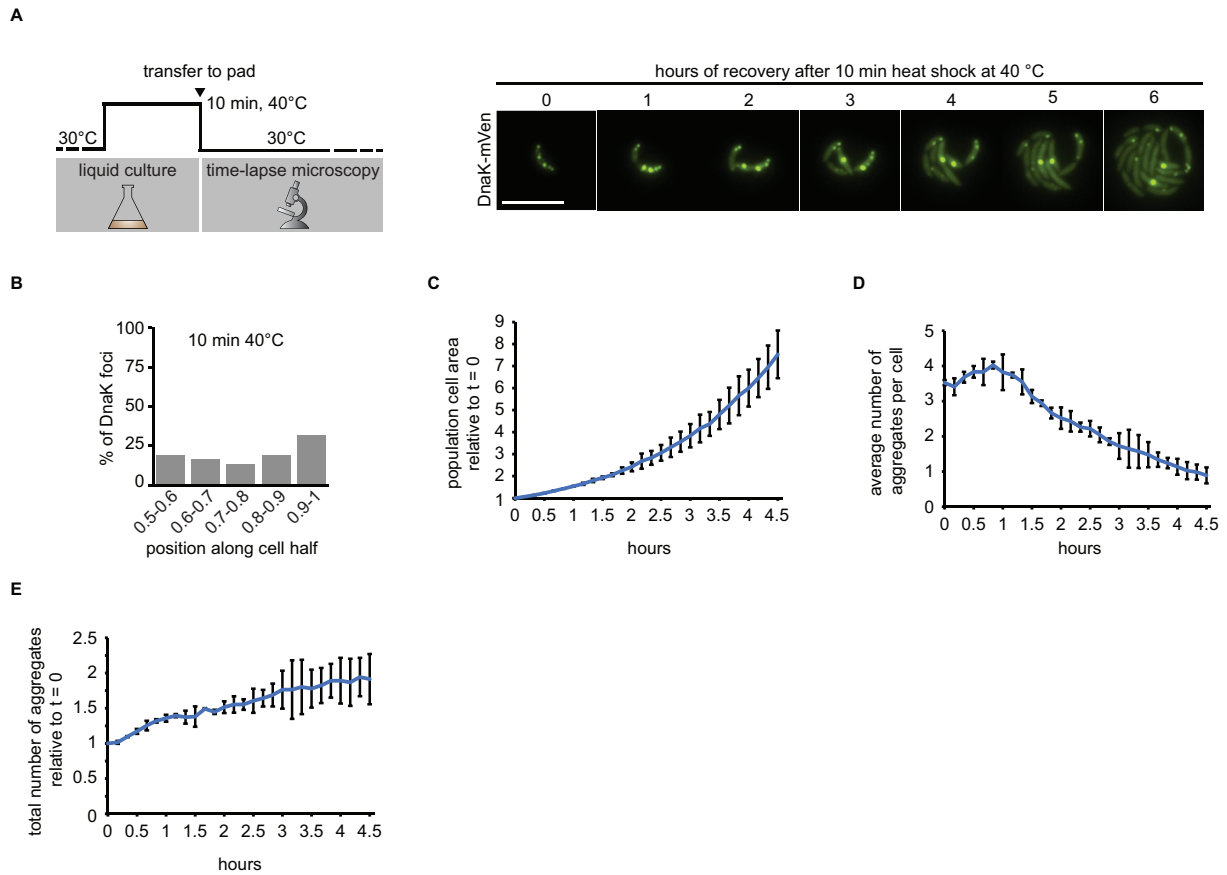
Supporting Information Table S2.

Supporting Information Movie S1.



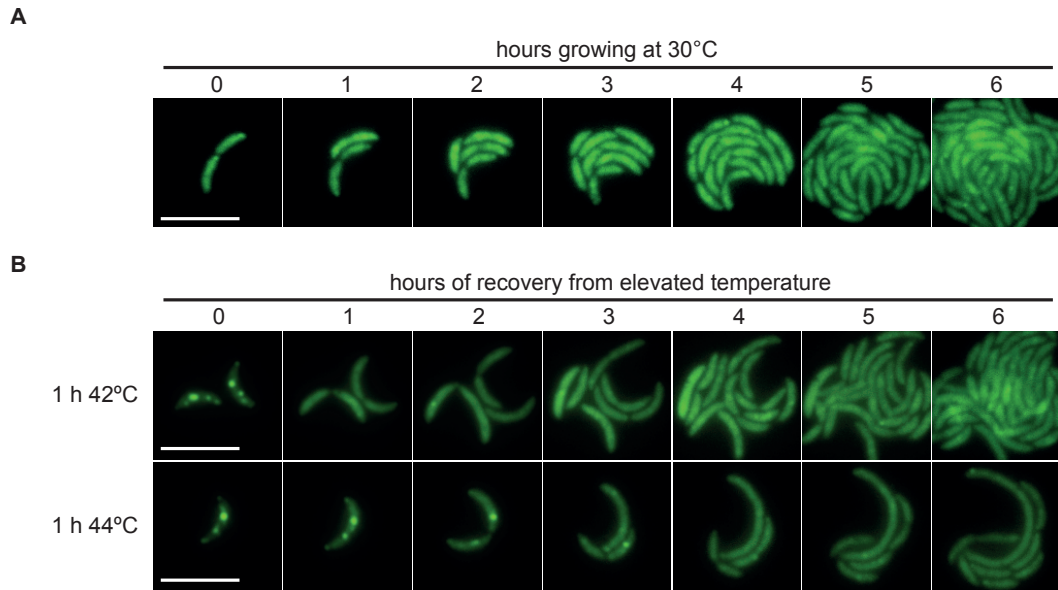
Supporting Information Figure S1. Viability and functionality of the fluorescent reporters used in this study.

(A) Spot assays showing resistance to exposure of 45°C of the wild type and strains bearing the indicated deletions or fusions in addition to DnaK-mVenus. (B) Microscopy images demonstrating localization of the small heat shock proteins sHSP1(CCNA_02341) and sHSP2(CCNA_03706) after 1 h at 40°C. (C) Fluorescence microscopy demonstrating localization of DnaK-mVenus, sHSP1-mCerulean, and the chromosome (stained with Hoechst 33258) after 1 h at 40°C. Scale bar is 5 μ m.



Supporting Information Figure S2. $\Delta clpB$ cells recovering from mild heat stress do not dissolve aggregates.

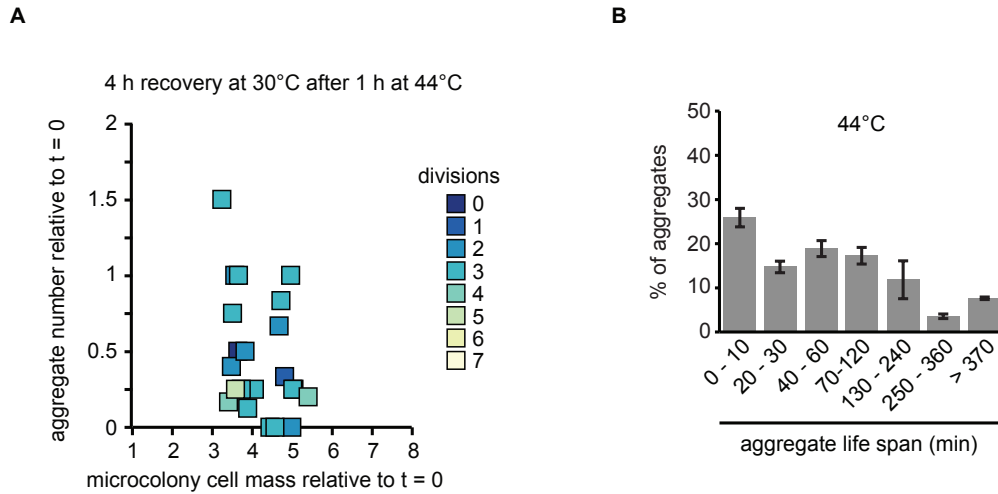
(A) Schematic of recovery experiment (left) and representative images from $\Delta clpB$ cell recovery after exposure to 40°C for 10 min. (B) Graph illustrating the position of DnaK-mVenus foci along five bins from midcell (0.5) to the cell pole (1) in $\Delta clpB$ cells after a 10 min heat shock at 40°C in liquid medium. Quantification based on 313 cells harboring 1056 aggregates. (C) Total population cell area increase relative to the area after stress exposure ($t=0$). (D) Average number of aggregates per cell over time. (E) Total number of aggregates present in the population over time normalized to time=0. Quantifications in (B-D) show the means of biological duplicates for which 19 microcolonies each were quantified. Error bars represent the standard deviation.



Supporting Information Figure S3. Representative time courses of cells continuously growing at 30°C or recovering from elevated temperature.

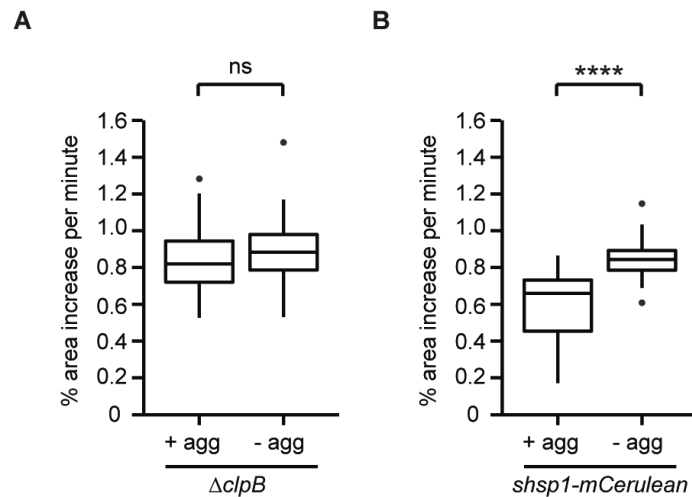
(A) Representative images of *C. crescentus* grown at 30°C in a heated microscopy chamber over a six hour period. (B) Representative images of *C. crescentus* grown at 30°C in a heated microscopy chamber during recovery from exposure to 42°C or 44°C over a six hour period.

Scale bar is 5 μm .














Supporting Information Figure S4. Growth and aggregate clearance in cells recovering from 1 h of exposure to 44°C.

(A) Scatter plot representing relative area increase, relative aggregate number normalized to the amount present at stress release, and the number of divisions of 22 cells and their progeny after four hours (the time at which the average area of the population has quadrupled) at 30°C after release from one hour of exposure to 44°C. (B) Quantification of aggregate life span in cells recovering from 44°C. Aggregates present or emerging in the first 400 min of a fluorescence time-lapse movie were tracked until 500 min. Images were acquired every 10 min. Quantifications show the means of biological duplicates for which at least ten microcolonies and 94 aggregates each were analyzed. Error bars represent standard deviations.



Supporting Information Figure S5. Growth rate comparisons between aggregate-harboring and aggregate-lacking cells.

(A) Growth rate distribution on a PYE agar pad at 30°C of second generation $\Delta clpB$ cells harboring (+ agg) or lacking (- agg) a single aggregate descending from a single aggregate-bearing mother cell. Before transfer to the pad, cells in liquid culture were exposed to 10 min at 40°C and left to recover at 30°C for two generations (as measured by OD₆₀₀) to obtain cells harboring only one aggregate. The growth rates of cells harboring one or no aggregates from 61 mother cells were recorded. Data from 40 stalked cells and 21 swarmer cells inheriting the single aggregate were pooled, and data from 40 stalked and 21 swarmer cells escaping inheritance of the aggregate were also pooled. (B) Growth rate distribution on a PYE agar pad at 30°C of second generation $shsp1-mCerulean$ expressing cells with or without a single large aggregate (Supporting Information Fig. S1B, C). Cultures were exposed to 40°C for 30 min and growth rates of cells descending from a single aggregate bearing mother cell were recorded as described in (A). The progeny of 22 mother cells was tracked and growth rates of stalked (7 cell pairs) and swarmer cells (15 cell pairs) were pooled. Unpaired t-tests were performed to test if the growth rate distributions significantly differed between cells with and without aggregates. ns (not significant), $p > 0.05$; ****, $p \leq 0.0001$.

original relative position in the mother cell	relative position in stalked daughter after cell division		
	closer to new pole	unchanged	closer to old pole
old pole 	 10% ¹ 16% ² 8% ³	 90% ¹ 94% ² 92% ³	N/A
old pole half 	 34% ¹ 58% ² 81% ³	 64% ¹ 42% ² 18% ³	 2% ¹ 0% ² 1% ³
midcell 	 71% ¹ 78% ² 66% ³	 26% ¹ 21% ² 30% ³	 3% ¹ 1% ² 4% ³

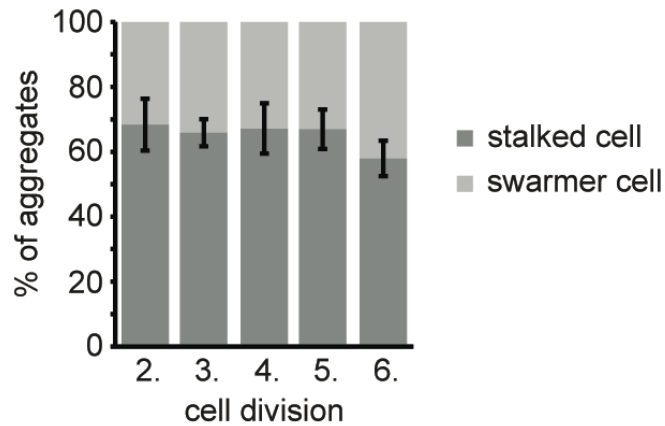
¹aggregates in $\Delta c/pB$ cells growing at 30°C after exposure to 40°C for 10 min (Fig. 6C)

²persistent aggregates in wild type cells (Fig. 4D) continuously exposed to 40°C (Supporting Information Fig. S8A)

³persistent aggregates in wild type cells (Supporting Information Fig. S4B) recovering at 30°C from 1 h at 44°C (Supporting Information Fig. S9A)

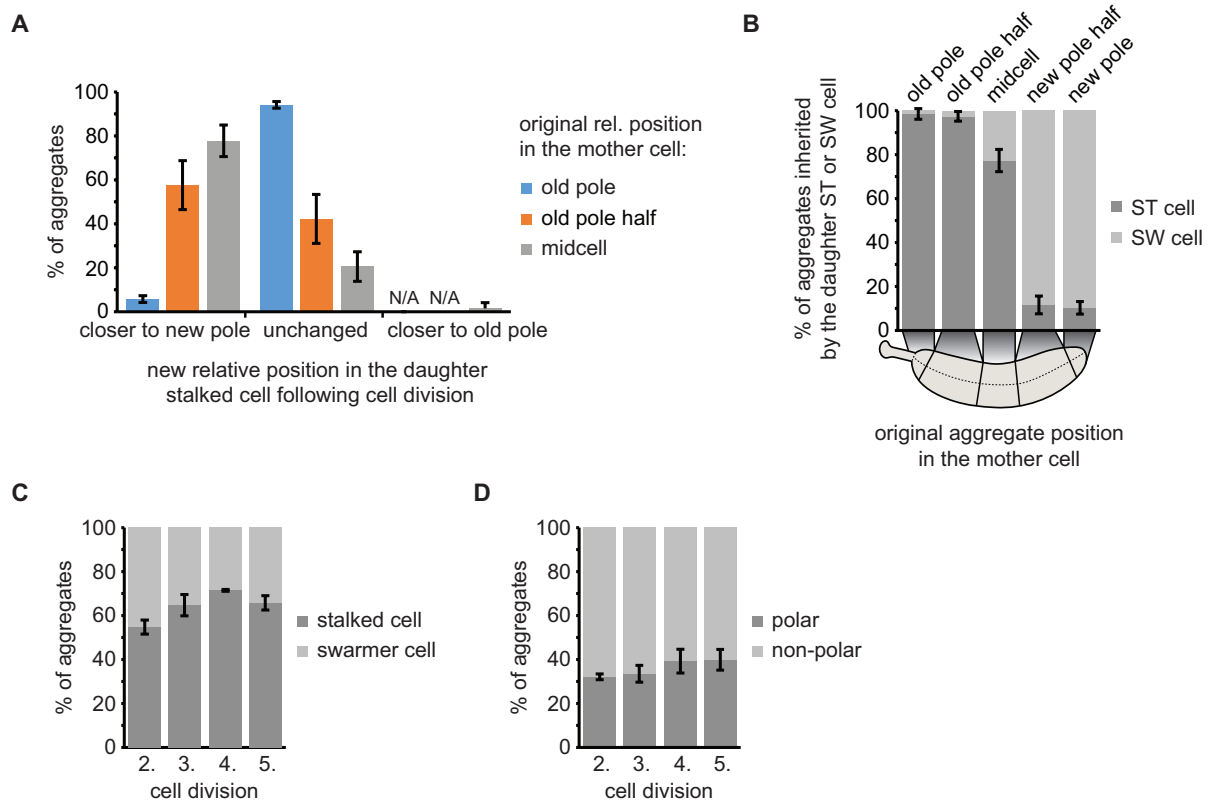
Supporting Information Figure S6. Schematic table summarizing how positional changes after cell divisions ranked by the position in the mother cell were quantified.

The table shows how aggregate inheritance was analyzed for generating Figure 6C and Supporting Information Fig. S8A, S9A. Percentage numbers represent the distribution of aggregate positional changes.



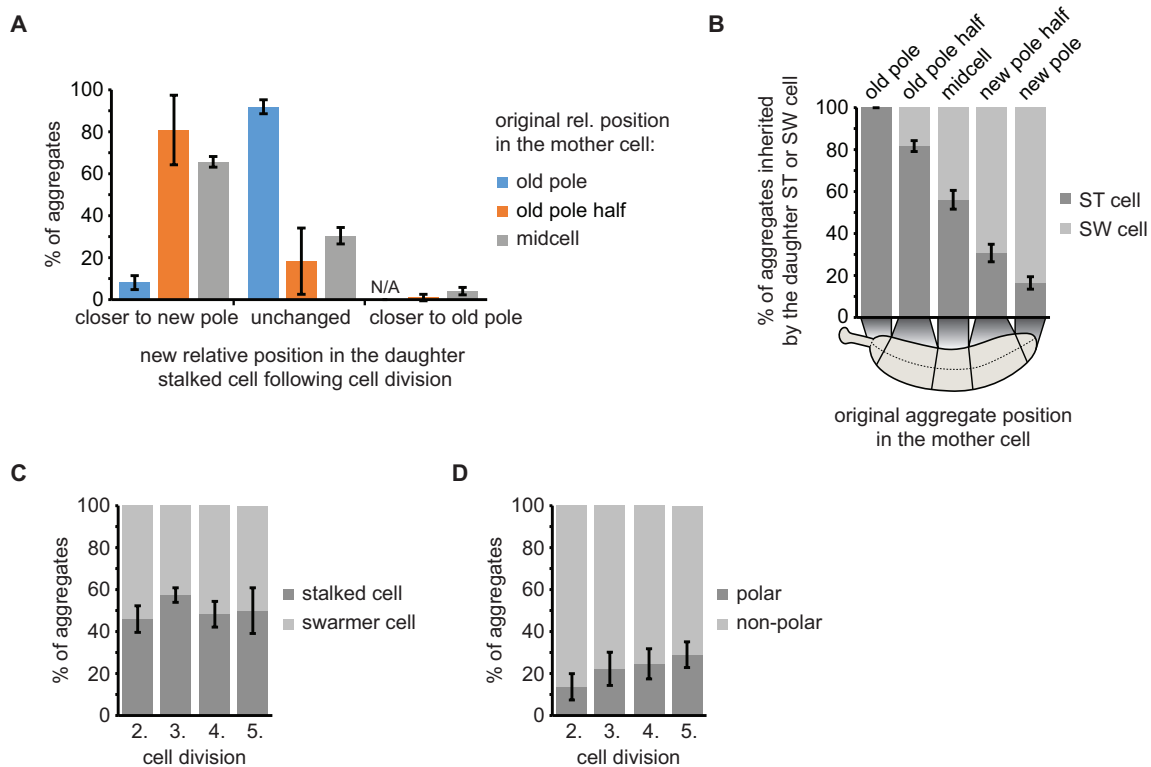
Supporting Information Figure S7. Inheritance of persistent protein aggregates that did not localize at a cell's old pole after the second cell division post stress in the $\Delta clpB$ background.

Aggregate inheritance was tracked in $\Delta clpB$ cells recovering from a 10 min heat shock at 40°C on a PYE agarose pad at 30°C. Aggregate position quantifications resulted from tracking the same population of aggregates from the second to the sixth division. Figure based on data presented in Fig. 6G. Percentage of aggregates inherited by the stalked or the swarmer daughter cell after the second to the sixth division excluding aggregates that localized at the old poles after the second division (Fig. 6H). Quantifications are based on biological triplicates for which at least 62 aggregates were tracked.



Supporting Information Figure S8. Inheritance of persistent protein aggregates in DnaK-mVenus cells continuously exposed to 40°C.

(A) Distribution of aggregates becoming closer to the new pole, remaining stationary or becoming closer to the old pole in the daughter stalked cell, ranked by position in the mother cell. (B) Proportion of aggregates inherited by either a swarmer or a stalked cell as function of their cellular position in the mother cell. (C) Percentage of aggregates inherited by the stalked or the swarmer daughter cell after the second to the fifth division. (D) Localization of aggregates tracked from the second to the fifth division. Aggregate position quantifications resulted from tracking the same population of aggregates from the second to the fifth division. Quantifications are based on biological triplicates for which at least 82 aggregates in at least 21 microcolonies each were tracked. For the quantifications in (A) and (B) the aggregate positional changes after each division were binned leading to at least 246 aggregate positional changes tracked per replicate. Error bars represent standard deviations.



Supporting Information Figure S9. Inheritance of persistent protein aggregates in DnaK-mVenus cells continuously exposed to 44°C.

(A) Distribution of aggregates becoming closer to the new pole, remaining stationary or becoming closer to the old pole in the daughter stalked cell, ranked by position in the mother cell. (B) Proportion of aggregates inherited by either a swarmer or a stalked cell as function of their cellular position in the mother cell. (C) Percentage of aggregates inherited by the stalked or the swarmer daughter cell after the second to the fifth division. (D) Localization of aggregates tracked from the second to the fifth division. Aggregate position quantifications resulted from tracking the same population of aggregates from the second to the fifth division. Quantifications are based on biological triplicates for which at least 96 aggregates in at least 85 microcolonies each were tracked. For the quantifications in (A) and (B) the aggregate positional changes after each division were binned leading to at least 288 aggregate positional changes tracked per replicate. Error bars represent standard deviations.

Supporting Information – Strain Construction

Extended description of plasmid construction.

Construct for fluorescence reporter tagging of *dnaK* at the native locus (pKJ936): A fragment containing the upstream homology region (UHR) made up of the last 600 bp of *dnaK* before the stop codon and encoding a GSG linker at the 3'-end was amplified using OFS193/318 from chromosomal DNA. The downstream homology region (DHR) encompassing the 665 bp downstream of the gene was amplified with OFS197/198 from chromosomal DNA. The fluorescence reporter encoding gene *mVenus* was amplified with OFS289/307. The fragments were assembled into *HindIII/EcoRI* restricted pNPTS138 by Gibson assembly (Gibson *et al.*, 2009).

Construct for fluorescence reporter tagging of *clpB* at the native locus (pKJ937): A fragment comprising the UHR encompassing the last 635 bp of *clpB* before the stop codon as well as encoding a GSG linker at the 3'-end was amplified using OFS287/288 from chromosomal DNA. The DHR containing the 601 bp downstream of *clpB* was amplified with OFS290/291. The fluorescence reporter encoding gene *mCerulean* was amplified with OFS289/307. The fragments were assembled into OFS285/286 amplified pNPTS138 by Gibson assembly.

Construct for fluorescence reporter tagging of *shsp1* (*CCNA_02341*) at the native locus (pKJ947): A fragment comprising the UHR encompassing 223 bp upstream of *shsp1* (*CCNA_02341*), the entire gene except for the stop codon and encoding a GSG linker at the 3'-end was amplified using OFS292/293 from chromosomal DNA. The DHR containing the 594 bp downstream of *shsp1* was amplified with OFS294/295. The fluorescence reporter encoding gene *mCerulean* was amplified with OFS289/307. The fragments were assembled into OFS285/286 amplified pNPTS138 by Gibson assembly.

Construct for fluorescence reporter tagging of *shsp2* (CCNA_03706) at the native locus (pKJ948): A fragment comprising the UHR encompassing 146 bp upstream of *shsp2* (CCNA_03706), the entire gene except for the stop codon and encoding a GSG linker at the 3'-end was amplified using OFS296/297 from chromosomal DNA. The DHR containing the 613 bp downstream of *shsp2* was amplified with OFS298/299. The fluorescence reporter encoding gene *mCerulean* was amplified with OFS289/307. The fragments were assembled into OFS285/286 amplified pNPTS138 by Gibson assembly.

Constructs for vanillate-dependent expression of mCherry-ELK16 from the chromosomal *vanA* locus (pKJ939): For the construction of pKJ939 the TP-linker-ELK16 encoding sequence was added to the 3'-end of *mCherry* by sequential PCRs in two steps. First *mCherry* was amplified using OFS308/309 and the resulting fragment was used as a template for an amplification with OFS308/310. The resulting fragment was restriction cloned into *NdeI/XbaI* cut pBVMCS-2 resulting in pKJ949. This construct was used as a template to amplify *mCherry-ELK16* which was then restriction cloned into *NdeI/SacI* cut pVCHYN-4 resulting in pKJ939.

Constructs for xylose-dependent expression of mCerulean-tagged endogenous aggregating proteins from the chromosomal *xyIX* locus (pKJ941-943): For the construction of pKJ941, pKJ942 and pKJ943, the endogenous genes were amplified from chromosomal DNA using OFS865/866, OFS869/870 or OFS880/881, respectively, and assembled with either OFS867/868, OFS871/868 or OFS875/879 amplified *mCerulean* into *NdeI/SacI* cut pXCHYN-1 by Gibson assembly.

Constructs for deleting chaperone and protease encoding genes (pKJ944-946): For making pKJ944 the UHR containing the 608 bp upstream and the first 15 bp of *ibpA* was amplified from genomic DNA using OFS795/796. The DHR containing the last 27 bp and the 586 bp downstream of *ibpA* was amplified with OFS797/798. The fragments were assembled with an

OFS801/802 amplified *rif^R*-cassette into *EcoRI/HindIII* cut pNPTS138 by Gibson assembly. In order to construct pKJ945 the UHR encompassing the 646 bp upstream and the first 15 bp of *ibpB* was amplified from genomic DNA using OFS809/817. The DHR containing the last 27 bp and the 612 bp downstream of *ibpB* was amplified using OFS811/818. The homology region were assembled with an OFS25/26 *tet^R*-cassette (pNPTS-*lon::tet^R*) (Leslie *et al.*, 2015) into *EcoRI/HindIII* cut pNPTS138 by Gibson assembly. For the generation of pKJ946 the UHR comprising the 606 bp upstream and the first 15 bp of *clpB* was amplified from genomic DNA using OFS803/807. The DHR encompassing the last 27 bp and the 537 bp downstream of *clpB* was amplified with OFS805/808. The homology region were assembled with an OFS25/26 amplified *tet^R*-cassette (pNPTS-*lon::tet^R*) (Leslie *et al.*, 2015) into *EcoRI/HindIII* cut pNPTS138 by Gibson assembly.

Constructs for ectopic overexpression of *dnaK*- and *dnaK(K70A)*-GSG-*mVenus* (pKJ950-951): For constructing pKJ950 *dnaK* was amplified from chromosomal DNA with OFS302/303 and assembled with OFS289/307 amplified *mVenus* into the OFS300/320 amplified vector pBVMCS-2 by Gibson assembly. In case of pKJ951 the mutation in *dnaK* was introduced by assembling two fragments by Gibson assembly which harbor the desired sequence alteration in the overlapping region. The fragments were amplified using OFS306/320 and OFS305/307, respectively, using pKJ951 as template.

Extended description of strain construction.

Fluorescence reporter tagging of *DnaK*, *ClpB*, *sHSP1* (CCNA_02341) and *sHSP2* (CCNA_03706) at the native locus (KJ952, KJ953, KJ967, KJ968): C-terminally tagging chromosomal chaperone genes with fluorescent reporter encoding sequences was achieved by a two-step recombination procedure (Skerker *et al.*, 2005). *C. crescentus* NA1000 was transformed with pKJ936 to generate KJ952. KJ952 was transformed with pKJ937 to generate

KJ953 with pKJ947 to generate KJ967 or with pKJ948 to generate KJ968. First integrants were selected for by plating on kanamycin-containing plates. Selected integrants were grown overnight in PYE medium lacking kanamycin and plated on 3 % sucrose containing plates. Clones being both sucrose-resistant and kanamycin sensitive were verified for plasmid excision and fluorescent reporter gene insertion at the correct locus by colony PCR and fluorescence microscopy.

Vanillate- and xylose-dependent expression of fluorescently tagged artificial and endogenous aggregating proteins from the chromosome (KJ955, KJ959-961): Plasmids encoding for fluorescently tagged artificial, endogenous aggregating and untagged fluorescent proteins under the control of *P_{vanA}* or *P_{xyLX}* were integrated through homologous recombination at the chromosomal *vanA* or *xyLX* site, respectively. Integrants were selected by the plasmid encoded antibiotic resistance and verified by colony PCR. KJ953 was transformed with pKJ939 to generate KJ955. For the generation of KJ959, KJ960 and KJ961, KJ952 cells were transformed with pKJ941, pKJ942 and pKJ943, respectively.

Wt DnaK- and DnaK(K70A)-GSG-mVenus overexpressing strains (KJ956, KJ957): *C. crescentus* NA1000 was transformed with the replicating plasmids pKJ950 and pKJ951 to obtain KJ956 and KJ957, respectively.

Chaperone and protease knockout strains (KJ962-966): Antibiotic-resistance marked knockouts of chaperone and protease encoding genes were obtained by two step recombination under constant exposure to the antibiotic against which the resistance cassette replacing the deleted gene sequence provides protection. KJ952 was transformed with either pKJ944, pKJ945, pKJ946 or pNPTS-*lon::tet^R* for the generation of KJ962, KJ963, KJ964 and KJ966, respectively. For constructing KJ965, KJ962 was transformed with pKJ945. Clones were verified by colony PCR.

Supporting Information References

Gibson, D.G., Young, L., Chuang, R.-Y., Venter, J.C., Hutchison, C.A., and Smith, H.O.

(2009) Enzymatic assembly of DNA molecules up to several hundred kilobases. *Nat Methods* **6**: 343–345.

Leslie, D.J., Heinen, C., Schramm, F.D., Thüring, M., Aakre, C.D., Murray, S.M., *et al.*

(2015) Nutritional Control of DNA Replication Initiation through the Proteolysis and Regulated Translation of DnaA. *PLOS Genet* **11**: e1005342.

Skerker, J.M., Prasol, M.S., Perchuk, B.S., Biondi, E.G., and Laub, M.T. (2005) Two-component signal transduction pathways regulating growth and cell cycle progression in a bacterium: a system-level analysis. *PLoS Biol* **3**: e334.